Hindawi
Security and Communication Networks
Volume 2023, Article ID 9864141, 1 page
https://doi.org/10.1155/2023/9864141

Retraction

Retracted: Design and Application of Art Education Communication Platform Based on Machine Vision

Security and Communication Networks

Received 20 June 2023; Accepted 20 June 2023; Published 21 June 2023

This article has been retracted by Hindawi following an investigation undertaken by the publisher [1]. This investigation has uncovered evidence of one or more of the following indicators of systematic manipulation of the publication process:

(1) Discrepancies in scope

(2) Discrepancies in the description of the research reported

(3) Discrepancies between the availability of data and the research described

(4) Inappropriate citations

(5) Incoherent, meaningless and/or irrelevant content included in the article

(6) Peer-review manipulation

The presence of these indicators undermines our confidence in the integrity of the article's content and we cannot, therefore, vouch for its reliability. Please note that this notice is intended solely to alert readers that the content of this article is unreliable. We have not investigated whether authors were aware of or involved in the systematic manipulation of the publication process.

Wiley and Hindawi regrets that the usual quality checks did not identify these issues before publication and have since put additional measures in place to safeguard research integrity.

We wish to credit our own Research Integrity and Research Publishing teams and anonymous and named external researchers and research integrity experts for contributing to this investigation.

The corresponding author, as the representative of all authors, has been given the opportunity to register their agreement or disagreement to this retraction. We have kept a record of any response received.

References

[1] B. Chen, Y. Lu, B. Tang, and W. Zhang, "Design and Application of Art Education Communication Platform Based on Machine Vision," *Security and Communication Networks*, vol. 2022, Article ID 1327190, 11 pages, 2022.

Hindawi
Security and Communication Networks
Volume 2022, Article ID 1327190, 11 pages
https://doi.org/10.1155/2022/1327190

Research Article

Design and Application of Art Education Communication Platform Based on Machine Vision

Bingyan Chen,[1] Yao Lu ,[2,3] Bangbei Tang,[4,5] and Wenya Zhang[6]

[1]*School of Design and Art, Henan University of Technology, Zhengzhou, Henan 450001, China*
[2]*Art Design College, Henan University of Urban Construction, Pingdingshan, Henan 467000, China*
[3]*School of Landscape Architecture, Dong-a University, Busan 612-022, Republic of Korea*
[4]*Department of Physiology, Army Military Medical University, Chongqing 400038, China*
[5]*School of Intelligent Manufacturing Engineering, Chongqing University of Arts and Sciences, Chongqing 402160, China*
[6]*College of Art, Henan Institute of Science and Technology, Xinxiang, Henan 453003, China*

Correspondence should be addressed to Yao Lu; 20172080@hncj.edu.cn

Received 23 June 2022; Accepted 20 July 2022; Published 13 August 2022

Academic Editor: Mohammad Ayoub Khan

There are some problems in the design and application of the art education exchange platform. In order to further analyze the relevant content of the art education exchange, based on machine vision theory, model calibration, and coordinate change are adopted to modify the original model, so as to obtain the optimized model. This model can be used to analyze the design and application of art education platform. Relevant studies show that, according to the coordinate parameter curve, the parameter α plays a promoting role on the coordinate value, while the parameter β plays a promoting role on the coordinate value first and then plays an inhibiting role. The parameter γ also promotes and inhibits coordinate values. The curve corresponding to parameter M_1 shows a gradual decline, and the curve of parameter M_2 has little influence on coordinate data. The curve corresponding to parameter M_3 also shows a linear trend of change. Through analysis, it can be seen that M_3 has the greatest influence on coordinate data. By using machine vision model to design and analyze the communication platform of art education, the changing trend of different indicators can be obtained. It can be seen from the analysis that both language and vocal music have obvious stability in the calculation process, which is an inherent attribute of communication platform. Finally, the accuracy of the optimization model is verified by analyzing and predicting the data. This research can provide theoretical support for the application of machine vision model in other fields.

1. Introduction

Machine vision has broad application prospects in different fields: graph optimization processing [1], sensors [2], sound source reconstruction [3], visual prediction [4], and pollution monitoring [5]. In view of a series of problems existing in the process of maize species analysis based on machine vision theory, the authenticity analysis method was introduced to obtain an optimized machine vision analysis model [6]. The optimization model checks the relevant laws of the corresponding species by extracting, analyzing, and optimizing corn data. In order to further analyze and predict the accuracy of corn-related parameters, the model was used to calculate the extracted data and obtain the corresponding prediction results. The accuracy of the model can also be verified by the results. This research can provide a reference for machine vision model in other fields of prediction. Tractor slippage and other related problems exist in the driving process. Through the introduction of optimized machine vision analysis theory and combined with relevant data analysis method, the slippage process of tractor was analyzed [7]. Relevant studies show that the model can predict and analyze the sliding process, and the analysis results can well reflect the actual situation of the tractor. This shows that the machine vision analysis model can well represent and study the tractor slip and other problems, so as

to provide theoretical support for the application of machine vision in other fields.

The above research mainly analyzes the application of machine vision in graphic processing and other aspects. In order to further improve the accuracy of art education communication platform, relevant theories of machine vision model were introduced, and the model of the relevant coordinate calibration, so that the results can be very good to meet the actual requirements. By using this model, the experimental results can be studied, and the model calculation and prediction show that the optimization model has a high application prospect. The model could play an important role in other areas.

2. Machine Vision

Machine vision is a rapidly developing branch of artificial intelligence. Machine vision is to use machines instead of human eyes to make measurements and judgments [8, 9]. Machine vision system uses machine vision products to convert the target to image signals and send them to a dedicated image processing system. The main features of machine vision are as follows: (1) The system selects workpiece of different sizes according to the operator, calls the corresponding visual program for size detection, and outputs the results; (2) the system can monitor the detection process by displaying images or dynamically view the detection results through the detection data displayed on the interface; (3) it has the function of timely and accurately sending out control signals and eliminating waste products to the wrong workpiece; (4) the model can display the detection screen in real time, and has the function of storing and viewing the image of the error workpiece in real time. The morphological information of the target is obtained and converted into digital signal according to the pixel distribution, brightness, color, and other information [10, 11]. The image system performs various operations on these signals to extract the characteristics of the target, and then controls the action of the equipment on-site according to the discriminant results.

Machine vision system has a wide range of applications in different fields, such as industry, agriculture, and biology. In order to analyze the relevant working principles and processes of the machine vision system, the working principle diagram of the machine vision system is obtained by summarizing and analyzing as shown in Figure 1. It can be seen from the figure that, firstly, the corresponding light source should be imported into the detected object, and the corresponding characteristic parameters can be obtained by analyzing the parameters of the detected object. Then the characteristic parameters are imported into the sensor of machine vision, and the corresponding data and parameters are obtained through the analysis of detection software such as camera and computer. Through further processing of data and parameters, it is imported into the control unit and finally returned to the detected data. Through such a cycle, the optimized results are finally obtained. Then the optimization results in accordance with the relevant criteria are derived.

2.1. Machine Vision Model Calibration. In the process of coordinate calibration, machine vision model is mainly analyzed from two aspects: coordinate transformation and corresponding coordinate optimization [12, 13].

2.1.1. Coordinate Conversion. Since the position of the camera is not fixed, the position and posture of 3d objects in the camera coordinate system may change. Because the error is mainly caused by the camera itself, the error parameter belongs to the internal parameter of camera calibration. To sum up, the parameters in the camera calibration solution model mentioned above include linear parameters and variable parameters, which are mainly affected by the camera itself. The external parameters are mainly determined by the $\{Hw\}$ selection. Therefore, it is necessary to establish the absolute coordinate system as a unified standard to describe the position and posture of objects in the objective world [14, 15]. Therefore, the absolute coordinate $\{Hw\}$ needs to be transformed into the camera coordinate $\{Hc\}$ by rotation and translation, and the corresponding specific change formula is as follows:

$$\begin{pmatrix} x_c \\ y_c \\ z_c \\ 1 \end{pmatrix} = \begin{pmatrix} R & t \\ 0^T & 1 \end{pmatrix} \begin{pmatrix} x_w \\ y_w \\ z_w \\ 1 \end{pmatrix}, \tag{1}$$

where R is the rotation matrix; t is the translation vector; x, y, and z are the corresponding coordinates. Where the specific coordinate of $\{Hc\}$ is $p_c = (x_c, y_c, z_c)^T$.

Through the above analysis, it can be seen that coordinate change has an impact on the calculation method, and then leads to the change of corresponding transformation results. Therefore, in order to further analyze the influences of three different coordinate transformations on specific transformation values, the influence curves of coordinate changes on transformation values are drawn as shown in Figure 2. It can be seen from Figure 2 that three different coordinates have different change curves, and the overall change trend is gradually rising. It can be seen from the transformation of parameter x coordinate that the transformation value corresponding to this curve is the largest among the three curves. With the increase of calculation time, the corresponding curve shows a gradually increasing trend, but when the corresponding time continues to increase, the curve will gradually tend to gentle. This shows that low time has a relatively large impact on the transformation value of parameters, while high time has a relatively small impact on the transformation value. It can be seen from the coordinate transformation curve of parameter y that when the time is low, its curve is basically consistent with the transformation value curve corresponding to x. With the gradual increase of time, the corresponding curve shows an approximate linear change trend, and the slope of the corresponding curve is constant. However, when the corresponding time reaches 460, the curve reaches the maximum value, while when the corresponding time exceeds 460, the curve gradually decreases. This shows that the

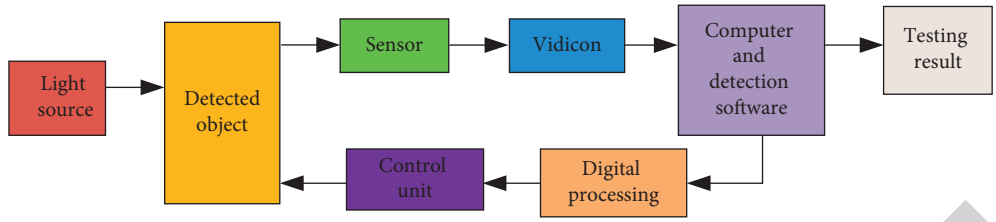

Figure 1: Machine vision systems work.

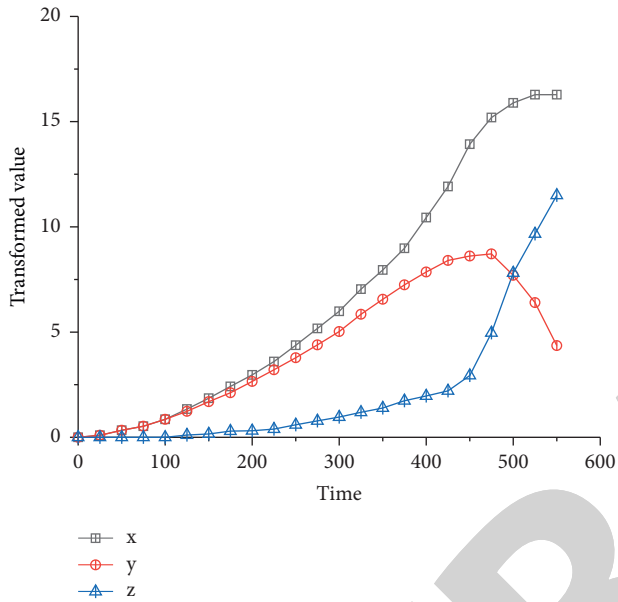

Figure 2: The curve of the effect of coordinate changes on transformation values.

different time will have different influence on the coordinate transformation value. As can be seen from the coordinate transformation curve of parameter z, the corresponding curve transformation value gradually increases with the gradual increase of time. It is worth explaining that before the time is 450, the change value of the curve is relatively small and approximately a constant change trend. When the time exceeds 450, the corresponding curve increases rapidly. The research shows that the higher the time, the greater the influence on the coordinate transformation value. Therefore, it can be seen from the analysis that the influence of parameter time on parameters has different forms. The corresponding rotation matrix change formula is as follows:

$$R(\alpha,\beta,\gamma) = \begin{pmatrix} 1 & 0 & 0 \\ 0 & \cos\alpha & -\sin\alpha \\ 0 & \sin\alpha & \cos\alpha \end{pmatrix} \times \begin{pmatrix} \cos\beta & 0 & \sin\beta \\ 0 & 1 & 0 \\ -\sin\beta & 0 & \cos\beta \end{pmatrix} \times \begin{pmatrix} \cos\gamma & -\sin\gamma & 0 \\ \sin\gamma & -\cos\gamma & 0 \\ 0 & 0 & 1 \end{pmatrix}. \tag{2}$$

α is the rotation of $\{Hw\}$ to $\{Hc\}$ about the X-axis; β is the rotation angle of $\{Hw\}$ to $\{Hc\}$ about the Y-axis; γ is the rotation of $\{Hw\}$ to $\{Hc\}$ about the Z-axis. The above parameters can be solved iteratively by the correlation algorithm, so as to obtain the corresponding model parameters. To sum up, the conversion relationship between absolute coordinates $\{Hw\}$ and camera coordinates $\{Hc\}$ can be obtained.

Through the corresponding image and data transformation formula we can see that different parameters have different effects on the transformation process and results. In order to quantitatively analyze the influence of three different parameters on coordinate indices, coordinate change curves under three different parameters were drawn through calculation and analysis as shown in Figure 3. It can be seen from the curves in the figure that the influences of the three parameters on the coordinate values have different trends. As the number of iterations increases, the parameter α shows a trend of gradual improvement, but its slope is relatively low. When the number of iterations exceeds 60, the slope of the corresponding curve is higher than that of the first stage. This indicates that the increase in the number of iterations will further increase the influence trend of parameter α. It can be seen from the change curve corresponding to parameter β that the change has a typical linear stage. As the number of iteration steps increases, the slope of the corresponding curve increases gradually, and when it exceeds the highest point, the curve falls rapidly, and the change trend of the falling curve is higher than that of the rising curve. This indicates that the coordinate value corresponding to the curve at this stage will produce a certain loss. As can be seen from the variation trend of parameter γ, the corresponding coordinate value of the curve decreases linearly as the number of iterations increases, and when it drops to the lowest point, the corresponding iteration number is about 6. As the number of iterations increases further, the slope of the curve increases rapidly at first and then slowly, indicating that in the process of increasing the number of iterations, the change of the curve will have a certain influence on the parameters. Therefore, in the application process, the proportion of the three parameters in different stages should be considered, so as to obtain the corresponding accurate coordinate value.

2.1.2. Coordinate Optimization. The transformation process of $\{Hc\}$ to $\{Hp\}$ can be described simply by small-hole imaging model [16, 17]. In the keyhole imaging model, point p is the next point $\{Hc\}$, and point p' is obtained by ray projection mapping with the optical center to the two-dimensional plane where $\{Hp\}$ is located. Therefore, the

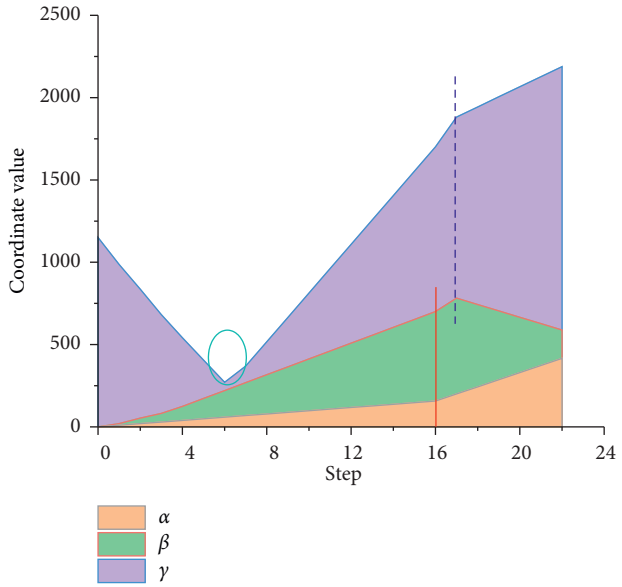

Figure 3: Graph of coordinate transformation under different parameters.

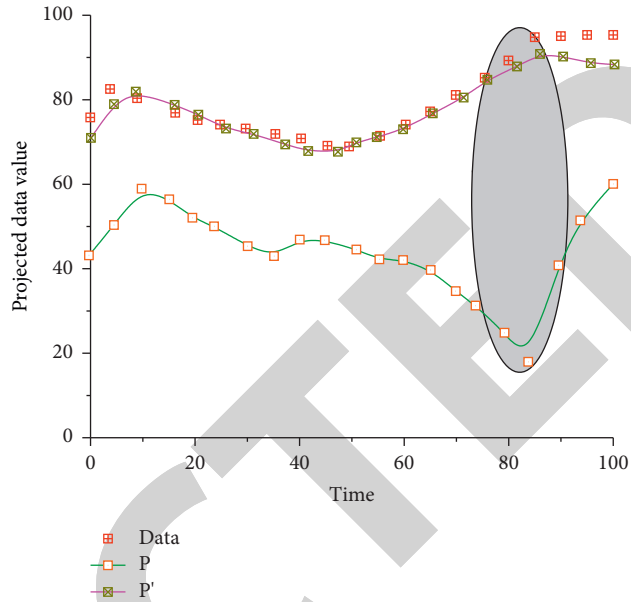

Figure 4: Optimization results of parameter p.

coordinate of P′ can be quickly obtained from the coordinate of P according to the simple similarity principle, and the corresponding calculation formula is as follows:

$$x_p = \frac{f}{z_c} x_c, \qquad y_p = \frac{f}{z_c} y_c. \tag{3}$$

The influence of parameter p on the optimization result is mainly through changing the corresponding x coordinate value and the corresponding y coordinate value and then changing the corresponding projection data. In order to further analyze the optimization results of parameter p, the curves corresponding to the original results and optimization results of parameter p are drawn through analysis as shown in Figure 4. It can be seen from the graph that the corresponding data shows a fluctuation trend with the increase of time, and its lowest point appears when the iteration time is about 50. When the iteration time exceeds 50, the slope of the corresponding curve gradually increases with the increase of iteration time, and then tends to be flat with the further increase of time, indicating that the corresponding curve data has a certain volatility. However, the curve corresponding to the original parameter p can only better describe the data change trend of the parameter under the action of a lower time. The change curve under the action of higher time has an opposite change trend in morphology, which indicates that parameter p can only describe the change pattern of curve under the action of lower time. As can be seen from the optimized parameter p curve, this curve can not only better describe the curve variation trend of parameter p under different time effects, but also better match the corresponding data at key nodes. This indicates that the optimized parameter can clearly describe the corresponding projection parameter and specific value, and can further illustrate the accuracy of the model corresponding to the optimized parameter p.

Transform the above formula into homogeneous coordinate and matrix form, the formula is as follows:

$$z_c \begin{pmatrix} x_p \\ y_p \\ 1 \end{pmatrix} = \begin{pmatrix} f & 0 & 0 & 0 \\ 0 & f & 0 & 0 \\ 0 & 0 & 1 & 0 \end{pmatrix} \begin{pmatrix} x_c \\ y_c \\ z_c \\ 1 \end{pmatrix}, \tag{4}$$

where f is the focal length of the camera. The corresponding relation between $\{Hc\}$ and $\{Hp\}$ is obtained.

According to the above analysis, it can be seen that different parameter f will have certain influence on the result of coordinate index. In order to more specifically analyze the influence of the change of parameter f on the coordinate index, the corresponding data of coordinate change under different parameter f are obtained through the calculation of the above formula, and the corresponding change curve is drawn as shown in Figure 5. It can be seen from the figure that the corresponding coordinate values of different parameter f have different trends. When the parameter $f = 1$, the corresponding curve shows a gradually increasing trend as the number of iterations gradually increases. And the increase between different data is basically the same, indicating that the curve approximately presents a linear change. When the parameter $f = 2$, with the gradual increase of the number of iterations, the corresponding coordinate data shows a gradual downward trend. However, when the number of iterations reaches 18, the curve increases suddenly, indicating that the influence of parameter f on the coordinate index shows different changes at this stage. When parameter $f = 3$, the corresponding coordinate data shows a trend of gradual decline as the number of iterations increases gradually.

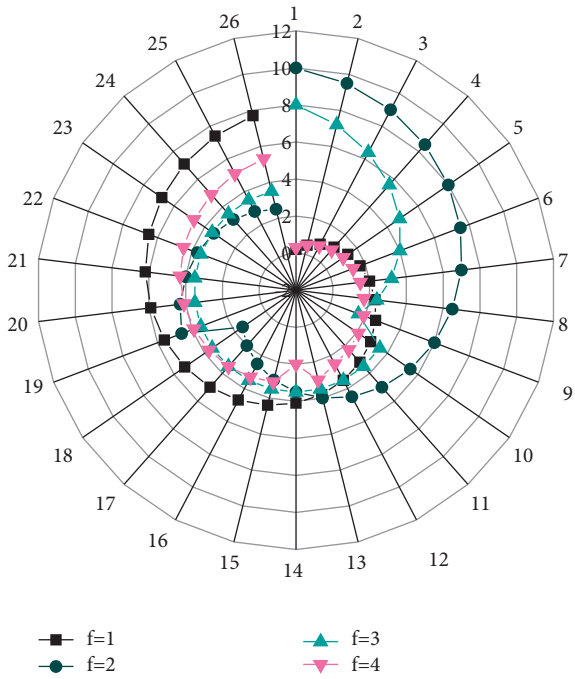

Figure 5: Influence of parameter f on coordinate indices.

However, when the number of iterations exceeds 8, the corresponding curve gradually tends to be stable. This indicates that the increase in the number of iterations has a relatively small impact on parameter $f = 3$. However, when parameter $f = 4$, the corresponding curve shows a gradual increase trend with the gradual increase in the number of iterations, and its overall increase trend is basically consistent with that of parameter $f = 1$. The change of camera focal length will lead to the difference between homogeneous coordinate and matrix coordinate, so that the result of coordinate optimization will change according to the difference of focal length. Further, the calculation results of rotation matrix are different, and finally different coordinate forms appear.

2.2. Graph and Pixel Coordinate Transformation. There is some deviation between the origin and coordinate axes of {*Hp*} and {*Hi*}, but they are generally considered to be in the same plane [18, 19]. Because the origin of {*Hp*} is in the center of the projected imaging image, and {*Hi*} is in pixels, it is used to read the picture in pixels into the computer for image processing.

In order to further analyze the specific process of graph processing under the effect of machine vision, we draw the graph processing process under different types as shown in Figure 6. Figure 6 shows that graph processing based on machine vision theory has a typical iterative effect. Firstly, the image is collected and the corresponding characteristic parameters are processed, and the specific data features are obtained through data processing. Then it is imported into the graphic size module, through which the image size is analyzed and optimized, and then it is imported into the dimension inspection module to check the defects of the graphic size. If it does not meet the requirements, it needs to be back to the image acquisition for further analysis. If it meets the requirements, the corresponding results will be imported into the defect detection; if the curve detection does not meet the requirements, it needs to continue the back generation. If it meets the requirements of defect detection and size detection, the image that meets the detection will be exported.

Assuming that the width of the pixel in the x direction is w and the height of the pixel in the y direction is h in the pixel coordinate system, the following formula can be obtained:

$$u = u_0 \frac{x_p}{w},$$
$$v = v_0 \frac{y_p}{h}. \tag{5}$$

The homogeneous matrix of the above formula is expressed as follows:

$$\begin{pmatrix} u \\ v \\ 1 \end{pmatrix} = \begin{pmatrix} \frac{1}{w} & 0 & u_0 \\ 0 & \frac{1}{h} & v_0 \\ 0 & 0 & 1 \end{pmatrix} \begin{pmatrix} x_p \\ y_p \\ 1 \end{pmatrix}, \tag{6}$$

thus, the transformation relation between {*Hp*} and {*Hi*} is deduced. Finally, the relationship between {*Hw*} and {*Hi*} is obtained, and the formula is as follows:

$$z_c \begin{pmatrix} u \\ v \\ 1 \end{pmatrix} = \begin{pmatrix} \frac{1}{w} & 0 & u_0 \\ 0 & \frac{1}{h} & v_0 \\ 0 & 0 & 1 \end{pmatrix} \begin{pmatrix} f & 0 & 0 & 0 \\ 0 & f & 0 & 0 \\ 0 & 0 & f & 0 \end{pmatrix} \begin{pmatrix} R & t \\ 0^T & 1 \end{pmatrix} \begin{pmatrix} x_w \\ y_w \\ z_w \\ 1 \end{pmatrix}$$
$$= M_1 M_2 \overrightarrow{p} = M_3 \overrightarrow{p}, \tag{7}$$

where M_1 is the internal parameter matrix of the camera; M_2 is the external parameter matrix; The coordinates of the origin op in {*Hi*} are (u_0, v_0); M_3 is the comprehensive matrix. After the camera calibration, the internal parameter is only related to the camera and has nothing to do with the world coordinate system. The external parameter matrix is related to the elements outside the camera, mainly related to the selected world coordinate system.

It can be seen from the above analysis that different matrix parameters will have an impact on specific matrix transformation data. Therefore, we summarize the influence of three different matrix parameters M_1, M_2, and M_3 on matrix change to obtain the change curve of corresponding matrix data as shown in Figure 7. It can be seen from Figure 7 that the matrix transformation values under three different parameters have different forms of

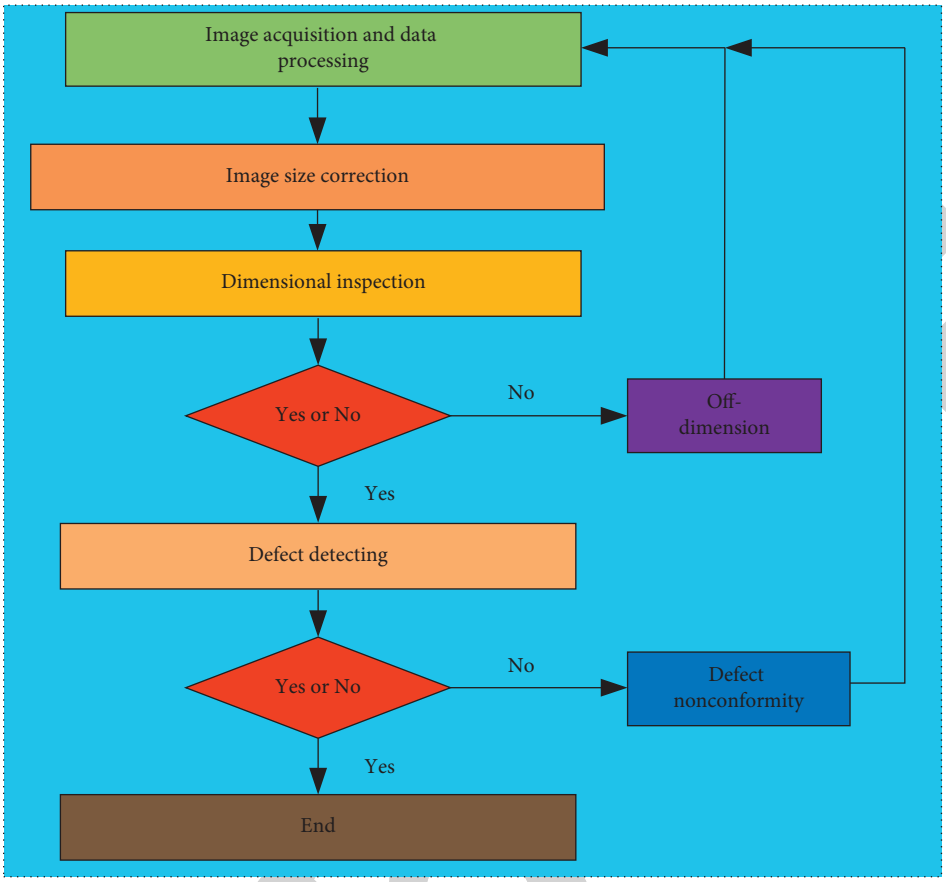

Figure 6: Graph processing flow chart.

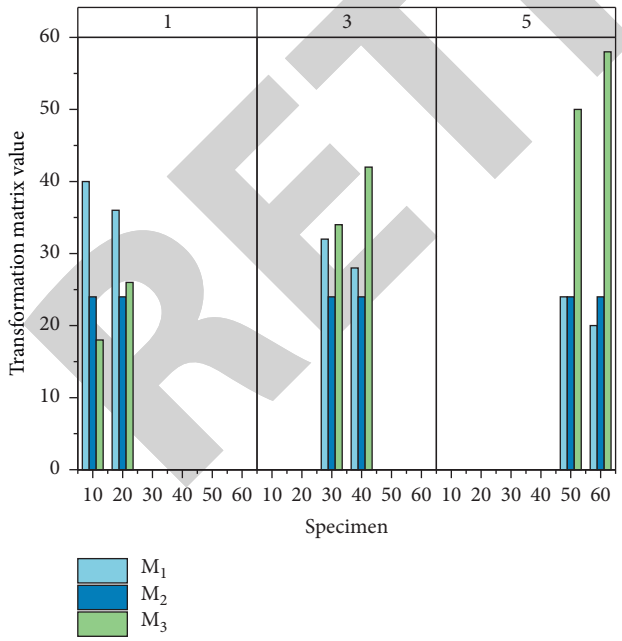

Figure 7: Matrix variation diagram.

change. As can be seen from the corresponding change results of parameters of M_1 matrix, with the gradual increase of the number of samples, the corresponding curve data shows a trend of gradual decline, and according to the change slope, it conforms to the change characteristics of linear. It can be seen from the transformation matrix data corresponding to parameter M_2 that, with the increase of the number of samples, the corresponding data shows a relatively gentle change trend, which indicates that the increase of samples does not have a great impact on the transformation matrix data. As can be seen from parameter M_3, with the increase of matrix samples, the corresponding matrix data shows a trend of gradual increase. Therefore, it can be seen from the variation trend of three different parameters $M_3 > M_2 > M_1$, and it can be divided into three different trends according to the number of different variation samples.

2.3. Machine Vision Model Optimization. The distortion of the central position of the imaging plane of the machine vision model is 0, and the distortion degree gradually increases with the outward direction of the optical center [20, 21]. The machine vision model is an ideal linear imaging model, while the keyhole imaging model only considers the ideal linear case, but the original image will be distorted excessively due to the calculation deviation and other reasons. In order to reduce the distortion of the image, it needs to be corrected in the original linear model. The mathematical model of radial distortion can be expressed by

Taylor's formula, and its specific mathematical distortion formula is as follows:

$$\begin{cases} x_0 = x\left(1 + k_1 r^2 + k_2 r^4 + k_3 r^6\right), \\ y_0 = y\left(1 + k_1 r^2 + k_2 r^4 + k_3 r^6\right). \end{cases} \tag{8}$$

In the above formula, (x, y) is the coordinate of the original image, (x_0, y_0) is the coordinate position of the optimized image, and r is the coordinate distance.

$$r^2 = x^2 + y^2. \tag{9}$$

The original machine vision model could not well represent the change process of test data, but the advantage of the optimized machine vision model is to improve the flexibility and automation degree of production. At the same time, in the process of mass calculation, using artificial vision to check product quality is inefficient and precision is not high, using machine vision detection method can greatly improve production efficiency and production automation degree. By using the above analysis and formula solution, the relationship between parameters x and y and the corresponding center radius r can be obtained. In order to further analyze the influence of x and y on the center radius r, we draw the change curve of the center radius under different parameters as shown in Figure 8. It can be seen from Figure 8 that parameters X and y show opposite variation trends, leading to different changes in corresponding results. Specifically, we can see that with the gradual increase of iteration time, the corresponding curve shows a typical two-stage change, and its change shows an obvious linear change. As the iteration time gradually increases, the curve first presents a trend of gradual decline, and when the iteration time exceeds 10, the corresponding curve presents a trend of gradual rise. The parameter y firstly rises slowly with the increase of time, and when it reaches the maximum value, it gradually decreases slowly with the increase of time, showing obvious symmetry. The curve corresponding to the calculated parameter center radius R shows a slow nonlinear increase at first, and then when it reaches the maximum value, the corresponding curve gradually decreases with the increase of iteration time, and the slope of the corresponding curve also shows a gentle decline. This shows that the curve corresponding to the center parameter radius R has obvious nonlinear characteristics. Therefore, the center radius corresponding to different parameters x and y has different changing trends. We should make targeted selection according to specific machine vision results.

The changes generated by the machine vision model can be expressed by two parameters p_1 and p_2 which are shown as follows:

$$\begin{cases} x_0 = x + 2p_1 y + p_1\left(r^2 + 2x^2\right), \\ y_0 = y + 2p_1 x + p_1\left(r^2 + 2y^2\right). \end{cases} \tag{10}$$

Finally, radial and tangential changes are added to the camera imaging model, and the specific formula is as follows:

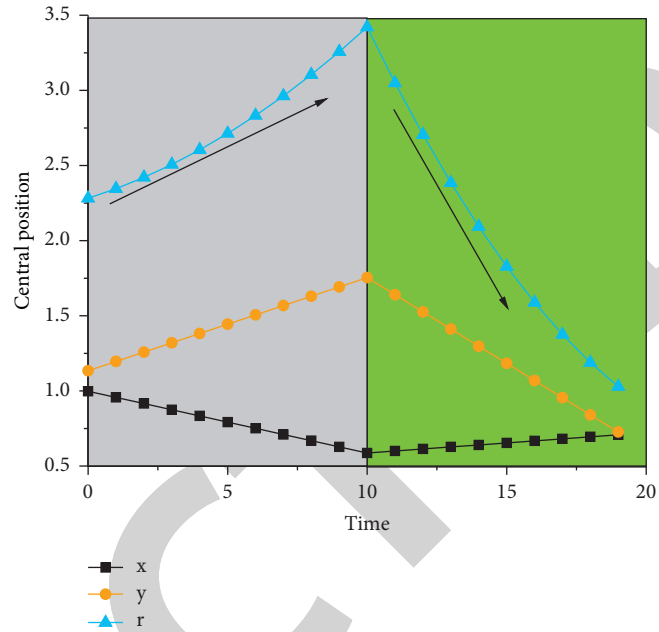

Figure 8: The change of the center radius r.

$$\begin{cases} x_0 = x\left(2 + k_1 r^2 + k_2 r^4 + k_3 r^6\right) + 2p_1 y + p_1\left(r^2 + 2x^2\right), \\ y_0 = y\left(2 + k_1 r^2 + k_2 r^4 + k_3 r^6\right) + 2p_1 x + p_1\left(r^2 + 2y^2\right). \end{cases} \tag{11}$$

Internal parameters include linear parameters fu, fv, u_0, and v_0, and variation parameters k1, k2, k3, p_1, and p_2. External parameters include R and t.

The coordinates corresponding to different parameters u and v show different changing trends, while the linear parameters fu, fv, and f have different changing forms. Therefore, in order to analyze the variation trend of parameter f, we drew linear parameter variation curves under different coordinates as shown in Figure 9. As can be seen from the curve in the figure, with the gradual increase of parameter u, the corresponding curve shows a gradual increase trend. The corresponding values are $f > fv >$ fu. With the gradual increase of parameter v, the corresponding curve also shows a linear increase trend, and the corresponding boundary and increased fluctuation range are relatively small. Therefore, we can select specific linear parameters when parameters u and v change, so as to describe the change of model coordinates pertinently.

3. Design and Application of Art Education Communication Platform Based on Machine Vision

3.1. Research Status of Art Education Exchange Platform. Art education exchange platform plays an important role in the field of culture, but with the development of culture, there are a series of problems in the field of art education: (1) Insufficient attention is paid to art education exchanges: with the rapid development of economy and society, the development of art education is relatively slow. As a result, art

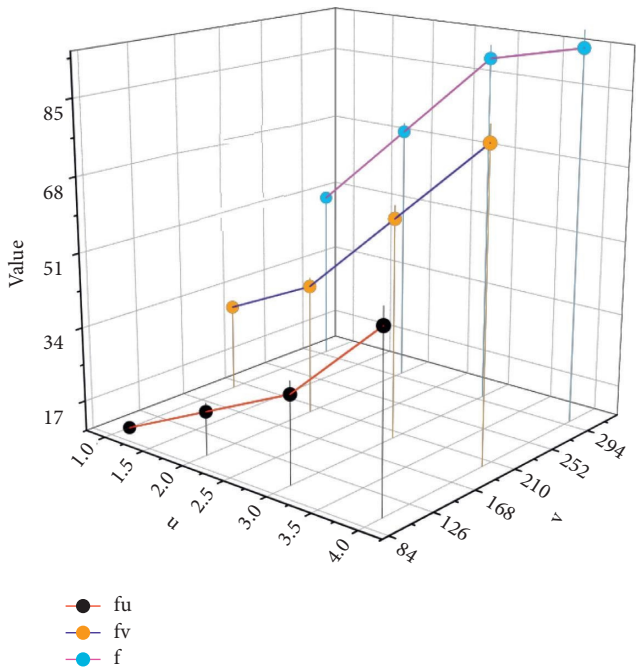

Figure 9: Linear parameter variation curve.

education lags far behind the pace of economic development and social progress, so we need to strengthen the importance of art and design. (2) The platform of art education and design is relatively single, which fails to promote the exchange of art and culture.

Art education exchange platform has different forms of expression. In order to better analyze the problems existing in art education exchange, we find six different targeted indicators to analyze the art exchange platform: 1 - language; 2 - text; 3 - dance; 4 - vocal music; 5 - painting; 6 - the martial arts. Through statistics and analysis, we obtained the distribution diagram of different indicators under the effect of this model. From Figure 10, we can see that different indicators have different table proportions on the art education communication platform. Among them, Wushu accounts for 34.04%, painting 21.28%, vocal music 17.02%, and dance 12.7%. The corresponding characters accounted for only 8.51%, and the language accounted for the least, only 6.38%. Through the different proportion, it shows that the communication and influence of different indicators on art education are different. We should fully consider the impact of different indicators on the communication platform of art education, so as to obtain accurate description and analysis.

3.2. Design of Communication Platform for Art Education by Machine Vision. Machine vision model has obvious application in different fields. In order to study its design and application in art education communication platform, we calibrate and change the coordinates of machine vision model [22]. Thus, the corresponding optimized machine vision model is introduced and imported into the art education design platform, so as to obtain the corresponding art communication platform design process based on the

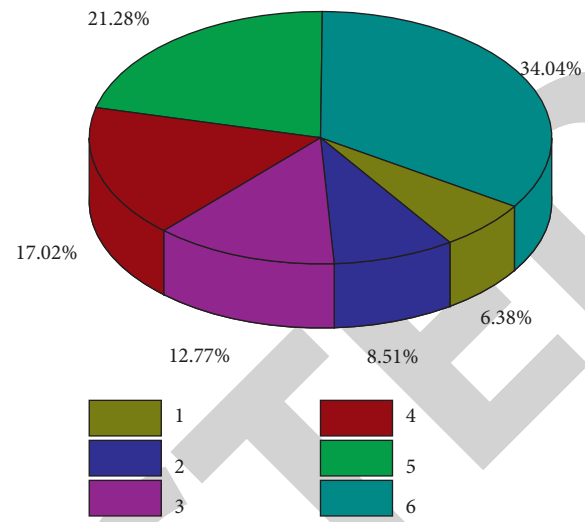

Figure 10: Distribution diagram of model indicators.

machine vision model as shown in Figure 11. As can be seen from the calculation process in the figure, the corresponding machine vision model is first imported into the corresponding module, and the corresponding art exchange platform data is obtained through the collection of the camera. Then the data of the art platform are imported into the art criteria for targeted judgment. If the results do not meet the requirements, the art platform needs to be optimized and then brought back to the art platform. If it meets the requirements, it will be entered into the education platform plate, and the iteration results of the corresponding education platform will be obtained through the optimization of relative indicators and determination of corresponding indicators, and the calculation results will be imported into the communication criteria for discrimination, and if it meets the requirements, it will be exported. If it does not meet the requirements, further study should be carried out. It is worth noting that the data collected by the camera can also be used to judge the communication between art education platforms, and then be imported into the communication criteria for the output of results.

The optimized machine vision model is used to analyze the art education exchange platform, and the histogram changes of the art education exchange platform under different factors are obtained, as shown in Figure 12. It can be seen from the changes in the figure that six different indicators have different manifestations under the calculation of machine vision model. As can be seen from indicator 1, with the gradual improvement of iterative steps, the proportion of language in art education is basically the same. This indicates that its influence on the art education communication platform under the machine vision model is relatively small, while index 2 decreases slowly at first and then increases gradually with the increase of iterations. This shows that the characters in art education have a relatively fluctuating trend under the action of machine vision model. With the increase of the number of iterations, index 3 firstly decreased rapidly and then increased slowly, and its fluctuation trend was higher than index 2. Index 4 remained

Figure 11: Design flow chart of art education platform based on machine vision model.

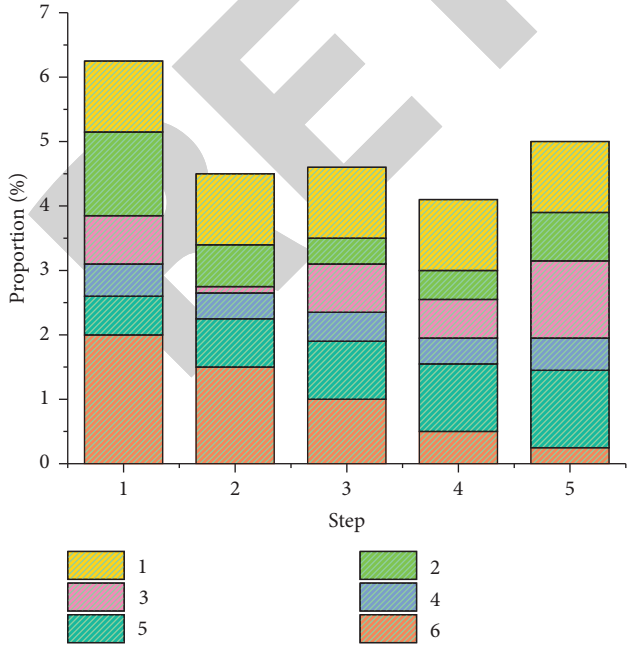

Figure 12: Bar chart of changes of art education platform under different factors.

constant with the increase of iteration steps. This indicates that the proportion of vocal music in art education has a constant influence on the communication platform of art education. This parameter can be used to analyze the model. With the increase of iteration steps, index 5 showed a significantly improved trend, while index 6 showed a gradually decreased trend with the increase of iteration times. The main reason for the different proportions of different indicators in the calculation of optimized machine vision model is that the proportions of art platform and education platform are different. As a result, the corresponding artistic criteria and educational criteria are used for unified analysis of indicators, resulting in different trends of different indicators.

4. Discussion

In order to further analyze the accuracy of the calculation results of the art education exchange platform under the effect of machine vision model, we need to make targeted prediction of the results of the art education exchange platform under the effect of this model. The model prediction curve under the effect of machine vision was obtained through analysis as shown in Figure 13. It can be seen

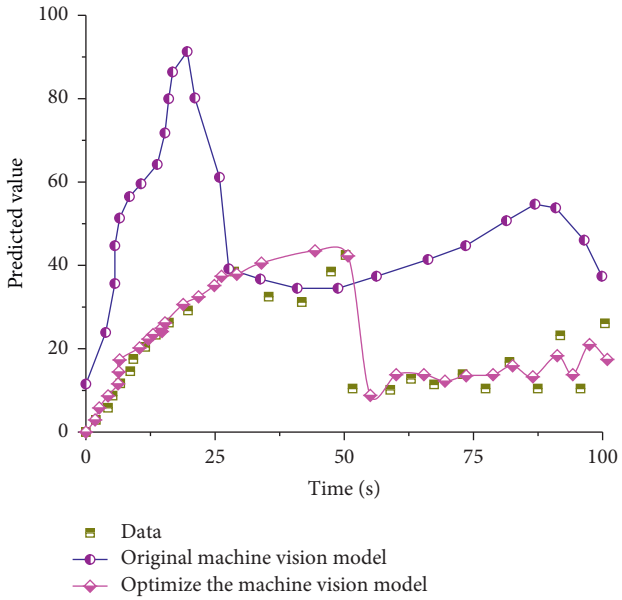

Figure 13: Machine vision model prediction diagram.

from the curves in the figure that the communication data of art education increases gradually over time, showing an approximate linear increase trend at first, then gradually declining and then rising slowly. With the gradual increase of the number, it shows an obvious trend of fluctuation. This means that the increase in time can lead to varying degrees of fluctuation in the data. It can be seen from the original machine vision model that the corresponding curve can better analyze the initial stage of art education data, while the description of the subsequent stage of the curve cannot be better, especially in the wave stage, which can only show a linear trend of change. However, the optimized machine vision model can not only describe the initial stage, but also better describe the fluctuation stage. Therefore, we can use this machine model to conduct targeted analysis and prediction of the art education exchange platform, so as to obtain accurate results. The optimized model can better analyze the first stage, mainly because the model fully considers the characteristics of the data changes in the first stage, and the linear characteristics of the curve in the first stage are obvious. For the second stage, the description of the model is relatively poor, mainly because the model only considers the main factors in the graph and platform communication process, and fails to fully consider the secondary factors, resulting in relatively poor calculation results.

5. Conclusion

(1) With the gradual increase of iteration time, the corresponding curves of parameter x and y show a relatively consistent trend in the initial stage. The difference between the two curves gradually increases. The corresponding curve of parameter z has a constant change in the initial stage and a rapid increase in the later stage of the curve.

(2) The parameter p of the original model cannot well describe the change curve of coordinates at a higher time. The optimized model parameters under the calibration of machine vision model can not only better analyze the change trend of the data, but also carry out accurate quantitative analysis of the data.

(3) As the number of iterations gradually increases, the corresponding coordinate data of parameter $f=1$ gradually increases. When $f=2$, the corresponding curve shows a trend of gradual decline. When the parameter $f=3$, the curve has a certain fluctuation.

(4) The curves corresponding to parameters x, y and center radius r all have obvious two-stage changes, and the trends of these two stages are opposite. This indicates that the change of time will have a certain influence on the center radius r value, and the specific characteristics of parameters should be considered comprehensively when selecting machine vision model parameters.

Data Availability

The data used to support the findings of this study are available from the corresponding author upon request.

Conflicts of Interest

The authors declare that they have no known competing financial interests or personal relationships that could have appeared to influence the work reported in this paper.

Acknowledgments

This work was supported by Henan Province Teaching Reform Project: Innovation and practice of talent training mode for new construction engineering majors in the digital age (NO.: 2021SJGLX529).

References

[1] Y. Guo, S. E. Aggrey, A. Oladeinde, J. Johnson, G. Zock, and L. Chai, "A machine vision-based method optimized for restoring broiler chicken images occluded by feeding and drinking equipment," *Animals*, vol. 11, no. 1, pp. 123–136, 2021.

[2] H. Kim, "CMOS image sensor for wide dynamic range feature extraction in machine vision[J]," *Electronics Letters*, vol. 57, no. 5, pp. 48–66, 2021.

[3] D. Li, H. Wu, Y. Zha, and W. Jiang, "A sound source reconstruction approach based on the machine vision and inverse patch transfer functions method," *Applied Acoustics*, vol. 181, no. 1, pp. 1081–1090, 2021.

[4] Q. Liao, C. Wei, Y. Li, L. Guo, and H. Ouyang, "Developing a machine vision system equipped with UV light to predict fish freshness based on fish-surface color," *Food and Nutrition Sciences*, vol. 12, no. 03, pp. 239–248, 2021.

[5] M. G. Pelletier, G. A. Holt, and J. D. Wanjura, "Cotton gin stand machine-vision inspection and removal system for plastic contamination: software design," *AgriEngineering*, vol. 3, no. 3, pp. 494–518, 2021.

[6] K. Tu, S. Wen, Y. Cheng et al., "A non-destructive and highly efficient model for detecting the genuineness of maize variety 'JINGKE 968′ using machine vision combined with deep learning," *Computers and Electronics in Agriculture*, vol. 182, no. 15, pp. 1060–1082, 2021.

[7] S. Zhu, L. Wang, Z. Zhu et al., "Measuring method of slip ratio for tractor driving wheels based on machine vision," *Agriculture*, vol. 12, no. 2, pp. 292–7625, 2022.

[8] M. T. Habib, M. J. Mia, M. S. Uddin, and F. Ahmed, "An explorative analysis on the machine-vision-based disease recognition of three available fruits of Bangladesh," *Vietnam Journal of Computer Science*, vol. 09, no. 02, pp. 115–134, 2022.

[9] J. Aab, V. I. Adamchuk, and J. Park, "Towards a machine vision-based yield monitor for the counting and quality mapping of shallots[J]," *Frontiers in Robotics and AI*, vol. 8, no. 3, pp. 510–523, 2021.

[10] J. Li, D. Mengu, and N. T. Yardimci, "Spectrally encoded single-pixel machine vision using diffractive networks[J]," *Science Advances*, vol. 7, no. 13, pp. 12–23, 2021.

[11] X. Li, H. Wu, X. Yang, P. Xue, and S. Tan, "Multiview machine vision research of fruits boxes handling robot based on the improved 2D kernel principal component analysis network," *Journal of Robotics*, vol. 2021, no. 12, Article ID 3584422, pp. 1–13, 2021.

[12] D. Liao, M. Yin, and H. Luo, "Machine vision system based on a coupled image segmentation algorithm for surface-defect detection of a Si3N4 bearing roller[J]," *Journal of the Optical Society of America*, vol. 39, no. 10, pp. 756–786, 2022.

[13] H. Liu, Z. Li, and R. Shen, "Point-of-Care pathogen testing using photonic crystals and machine vision for diagnosis of urinary tract infections[J]," *Nano Letters*, vol. 21, no. 7, pp. 7562–7593, 2021.

[14] Y. Majeed, M. Karkee, and Q. Zhang, "Development and performance evaluation of a machine vision system and an integrated prototype for automated green shoot thinning in vineyards[J]," *Journal of Field Robotics*, vol. 10, no. 1, pp. 36–46, 2021.

[15] B. B. Nair, S. Krishnamoorthy, and M. Geetha, "Machine vision based flood monitoring system using deep learning techniques and fuzzy logic on crowdsourced image data[J]," *Intelligent Decision Technologies*, vol. 28, no. 9, pp. 1–14, 2021.

[16] L. Nazari, M. Shaker, and A. Karimi, "Identification of sorghum genotypes using a machine vision system[J]," *Journal of Food Process Engineering*, vol. 5, no. 10, pp. 286–295, 2021.

[17] M. J. Park and H. J. Kim, "Deep learning machine vision system with high object recognition rate using multiple-exposure image sensing method[J]," *Journal of Sensor Science and Technology*, vol. 16, no. 2, pp. 342–372, 2021.

[18] L. Shi, J. Tan, S. Xue, and J. Deng, "Inspection method of rope arrangement in the ultra-deep mine hoist based on optical projection and machine vision," *Sensors*, vol. 21, no. 5, pp. 1769–1801, 2021.

[19] B. Xue and Z. Wu, "Key technologies of steel plate surface defect detection system based on artificial intelligence machine vision," *Wireless Communications and Mobile Computing*, vol. 2021, no. 12, Article ID 5553470, pp. 1–12, 2021.

[20] D. Zhang and Z. Guo, "Mobile sentry robot for laboratory safety inspection based on machine vision and infrared thermal imaging detection," *Security and Communication Networks*, vol. 2021, no. 3, Article ID 6612438, pp. 1–16, 2021.

[21] X. Zhang, X. Hu, and H. Li, "A speed inference planning of groove cutting robot based on machine vision and improved fuzzy neural network[J]," *Journal of Intelligent and Fuzzy Systems*, vol. 17, no. 7, pp. 1–14, 2021.

[22] C. Zhao, H. Ding, G. Cao, and Y. Zhang, "A new method for detecting compensation hole parameters of automobile brake master cylinder based on machine vision," *Journal of Advanced Transportation*, vol. 2021, no. 3, Article ID 8864679, pp. 1–14, 2021.